19. Montefort S, Roche WR, Howarth PH, et al. Intercellular adhesion molecule-1 (ICAM-1) and endothelial leucocyte adhesion molecule-1 (ELAM-1) expression in the bronchial mucosa of normal and asthmatic subjects. *Eur Respir J* 1992;5:815–823.
20. Keelan ETM, Licence ST, Peters AM, et al. Characterization of E-selectin expression in vivo with use of a radiolabeled monoclonal antibody. *Am J Physiol* 1994;266:H279–H290.
21. Mountford PJ, Kettle AG, O'Doherty MJ, Coakley AJ. Comparison of technetium-99m-HMPAO leukocytes with indium-111-oxine leukocytes for localizing intraabdominal sepsis. *J Nucl Med* 1990;31:311–315.
22. Roddie ME, Peters AM, Danpure HJ, et al. Inflammation: imaging with Tc-99m HMPAO-labeled leukocytes. *Radiology* 1988;166:767–772.
23. Reynolds JH, Graham D, Smith FW. Imaging inflammation with ^{99m}Tc-HMPAO-labeled leucocytes. *Clin Radiol* 1990;42:195–198.
24. Leeuwenberg JFM, Smeets EF, Neefjes JJ, et al. E-selectin and intercellular adhesion molecule-1 are released by activated human endothelial cells in vitro. *Immunology* 1992;77:543–549.
25. Norris P, Poston RN, Thomas S, Thornhill M, Hawk J, Haskard DO. The expression of endothelial leukocyte adhesion molecule-1 (ELAM-1), intercellular adhesion molecule-1 (ICAM-1) and vascular cell adhesion molecule-1 (VCAM-1) in experimental cutaneous inflammation: a comparison of ultraviolet B erythema and delayed hypersensitivity. *J Invest Dermatol* 1991;96:763–770.
26. Serafini AN, Garty I, Vargas-Cuba R, et al. Clinical evaluation of a scintigraphic method for diagnosing inflammations/infections using indium-111-labeled nonspecific human IgG. *J Nucl Med* 1991;32:2227–2232.
27. Becker W, Schomann E, Fischback W, et al. Comparison of ^{99}Tc-HMPAO and ^{111}In-oxine-labeled granulocytes in man: first clinical results. *Nucl Med Commun* 1988;9:435–447.
28. Hnatowich DJ. Antibody radiolabeling, problems and promises. *Nucl Med Biol* 1990;17:49–55.
29. Oyen WJG, Claessens RAMJ, van Horn JR, et al. Scintigraphic detection of bone and joint infections with indium-111-labeled nonspecific polyclonal human immunoglobulin G. *J Nucl Med* 1990;31:430–412.
30. Sasso D, Gionfriddo M, Syrbu S, Smilowitz H, Thrall R, Weiner R. Early detection of ARDS using In-111 labeled anti-intercellular adhesion molecule-1 in a rat model [Abstract]. *J Nucl Med* 1995;36(suppl):159P.
31. Hiroe M, Ohta Y, Miyasaka M, et al. Myocardial uptake of radiolabeled monoclonal anti-intercellular adhesion molecule-1, antibody in detecting acute myocardial infarction of rat [Abstract]. *J Nucl Med* 1993;34(suppl):66P.
32. Hiroe M, Ohta Y, Amano J, et al. Uptake of indium-111 labeled anti-intercellular adhesion molecule-1 antibody in early detection of lung allograft rejection in rats [Abstract]. *J Nucl Med* 1994;34(suppl):239P.
33. Ohtani H, Strauss HW, Southern JF, et al. Imaging of intercellular adhesion molecule-1 induction in rejecting heart: a new scintigraphic approach to detect early allograft rejection. *Transplant Proc* 1993;25:867–869.
34. Doerschuk CM, Beyers N, Coxson HO, et al. Comparison of neutrophil and capillary diameters and their relation to neutrophil sequestration in the lung. *J Appl Physiol* 1993;74:3040–4045.
35. Ussov WY, Peters AM, Hodgson HJF, Hughes JMB. Quantification of pulmonary uptake of indium-111 labeled granulocyte in inflammatory bowel disease. *Eur J Nucl Med* 1994;21:6–11.
36. McAfee JG, Gagne GM, Subramanian G, et al. Distribution of leukocytes labeled with In-111 oxine in dogs with acute inflammatory lesions. *J Nucl Med* 1980;21:1059–1068.
37. Sasso D, Gionfriddo M, Thrall RS, Syrbu S, Smilowitz HM, Weiner RE. Biodistribution of antibody directed against intracellular adhesion molecule-1 in normal rats [Abstract]. *Am J Respir Crit Care Med* 1995;171(suppl):A70.

HMPAO as a Regional Cerebral Blood Flow Tracer at High Flow Levels

Roderick Duncan, James Patterson and I. Mhairi Macrae

Departments of Neurology and Clinical Physics, Institute of Neurological Sciences, Southern General Hospital NHS Trust, Glasgow; and Wellcome Surgical Institute, University of Glasgow, Glasgow, Scotland

HMPAO is being used extensively to image rCBF during focal seizures in humans. It is, however, theoretically possible that backdiffusion of tracer causes retention to fall as flow rises at high levels. **Methods:** We used a double label ^{99m}Tc-HMPAO/^{14}C-IAP autoradiographic technique to compare HMPAO retention and regional cerebral blood flow in penicillin induced focal seizures in rats. **Results:** Using this protocol, flows of up to 717 ml/100 g per min were observed. The same pattern of uptake was seen on IAP and HMPAO autoradiographs, with the exception of relatively high HMPAO uptake in the choroid plexus, in the fissures and, in one animal only, the supramammilary nucleus. Correlation of HMPAO retention and blood flow showed a linear relationship up to 200 ml/100 g per min in all animals. HMPAO retention then showed a falloff in its rise with blood flow, but was still increasing, even at the highest flows seen. At 700 ml/100 g/min, HMPAO retention was 20% of that expected from a linear relationship. **Conclusion:** HMPAO is a suitable tracer of rCBF at high flows and is unlikely to produce anomalous images in human focal seizures.

Key Words: epilepsy; penicillin; rCBF; technetium-99m-HMPAO

J Nucl Med 1996; 37:661–664

HMPAO (*1*) is a lipophilic compound that can be labeled with ^{99m}Tc and used as a tracer of regional cerebral blood flow (rCBF). After intravenous injection, it crosses the blood-brain barrier freely. Thereafter, it becomes less lipophilic and less able to re-cross cellular membranes and the blood-brain barrier. Therefore, the distribution of HMPAO in the brain reflects rCBF and remains stable for some hours.

The brain distribution of microspheres and ^{99m}Tc-HMPAO correlate well in the dog (*2*), and previous autoradiographic studies using iodoantipyrine (IAP) have also shown good agreement (*3,4*). Initial uptake in the normal human brain appears to be proportional to rCBF (*5*), and to correspond well with rCBF as shown by other in vivo methods, such as ^{133}Xe (*6,7*) and PET (*8,9*).

The conversion of HMPAO to a less lipophilic compound takes place with an exponential half life of 40 sec. Thus, at high flow rates, there is a backdiffusion effect, causing HMPAO uptake to underestimate flow. Lassen et al. (*5*) proposed a correction which can partially compensate for this effect.

Ictal HMPAO-SPECT is now being used extensively to localize epileptic foci prior to surgical resection (*10,11*). Although human data is scant, animal work has shown ictal rises in rCBF in generalized seizures of up to 900% (*12*). At these extremely high flow rates (up to 1000 ml/100 g per min in absolute terms), it is important to verify that HMPAO retention in neurones does not begin to fall as flow rises, as the same ^{99m}Tc activity might then be seen at two different flow rates. A recent publication (*13*) has underlined the need to verify the accuracy of the technique in specific pathological situations.

This study aims to compare HMPAO uptake with rCBF as measured by IAP uptake over the large range of flows achieved using the penicillin model of focal epilepsy in the rat.

Received Feb. 10, 1995; revision accepted Jul. 14, 1995.

For correspondence or reprints contact: Roderick Duncan, MD, Department of Neurology, Institute of Neurological Sciences, Southern General Hospital, Glasgow, Scotland G51 4TF.

METHODS

Adult male Sprague-Dawley rats (480 ± 21 g) were used, five for nonseizure and five for seizure studies.

Induction of Focal Motor Seizures Using Intracortical Injection of Penicillin

The rats were anesthetised with halothane and nitrous oxide using a plastic face mask. Cannulae were inserted into both femoral arteries and veins. The animal was placed in a plaster of paris hip brace for restraint, and a 1-mm burr hole was made 2-mm anterior and lateral to bregma, a hole sufficiently deep to expose a 0.5-mm disc of dura. The skin was then resutured.

One venous catheter was connected to the syringe pump containing 1.85 MBq ^{14}C-IAP in 1.5 ml, the other to a syringe containing 320 MBq ^{99m}Tc-HMPAO in 1 ml. One arterial catheter was used to monitor intra-arterial pressure and the other to sample blood during the IAP procedure.

After checking blood pressure and gasses, the burr hole was re-exposed. A fine needle attached to a 500 μl microsyringe was inserted into the cortex through the dura to a depth of 1.5 mm from the outer dural surface. Two hundred units of penicillin in 20 μl pH-balanced artificial CSF was injected. Control animals were injected with 20 μl artificial CSF adjusted to the pH of the penicillin solution. The scalp wound was resutured, and the anesthesia discontinued.

The experiment was timed from the first observed movement in nonseizure animals, and from the onset of twitching of the whiskers contralateral to the craniotomy in the rats who had seizures. Seven minutes after this point, after thorough mixing, 320 MBq ^{99m}Tc-HMPAO were injected intravenously in 1-ml increments over 1 min. Three minutes were allowed between the injection of HMPAO and the start of the IAP procedure to allow time for any backdiffusion of HMPAO to occur. After 11 min of seizure activity, the time at which the animals had been in clinical steady state for several minutes, the IAP procedure was performed. The procedure and the method of rCBF calculation are described in detail by Sakurada et al. (*14*) and Tamura et al. (*15*). The 1.85 MBq ^{14}C-IAP was administered as a ramped infusion over 30 sec. During the infusion, 15–18 timed arterial blood samples were collected in pre-weighed filter paper discs. The rats were killed by decapitation at the end of the infusion. The blood samples were left for 4 days to allow ^{99m}Tc activity to disappear, then placed in a scintillation counter, counted three times and the counts averaged. The concentration of ^{14}C in blood was calculated from the detected radioactivity and the sample weight.

Immediately following the IAP procedure, the brain was quickly removed and frozen in isopentane at −42°C, and 20-μm coronal sections were collected for autoradiography. Three consecutive sections in every 13 were mounted on cover slips. Within 1 hr of decapitation, the sections were apposed to autoradiographic film for 4 hr, together with a set of six ^{14}C standards of activities (90–703 kBq/g). This enabled us to measure the technetium levels in ^{14}C equivalent units. After a similar gap of 4 days, the sections were reapposed to ^{14}C sensitive film for 14 days, this time with a lower activity set of twelve ^{14}C standards ranging from 1.6–54.7 kBq/g, to produce the [^{14}C]IAP autoradiograph.

Quantitative autoradiography was carried out on both films using a Quantimet 970 densitometer (Cambridge Instruments, Cambridge, U.K.). The structures measured were: frontal, cingulate, parietal, auditory and visual cortex, subcortical white matter, caudate nucleaus, globus pallidus, septal nucleus, amygdaloid nucleaus, medial and lateral habenula, ventral, dorsomedial and lateral thalamic nuclei, entopeduncular nucleus, hippocampus, substantia nigra, inferior colliculus, pontine reticular formation and cerebellum. Each structure was measured on three adjacent sections and the measurements were averaged. Structures were measured at the same position on the same section in both the IAP and HMPAO films. The standards were measured before and after measurement of the structures.

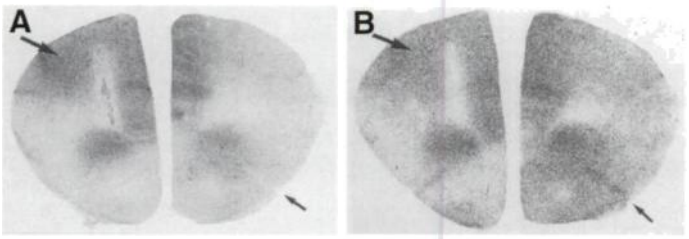

FIGURE 1. (A) IAP and (B) HMPAO images. Coronal section through the frontal lobe in animal 6, showing increased HMPAO and the seizure focus (large arrow). There is low HMPAO and IAP uptake in the area of the needle track, surrounded by an area of high uptake which extends into the neighboring and contralateral cingulate cortex. On the IAP film, uptake in the rhinal fissure is lower than that in the surrounding cortex, whereas on the HMPAO film, it is higher (small arrows).

Regional cerebral blood flow was calculated, as described by Sakurada et al. (*14*), from the arterial IAP curve and the local tissue ^{14}C concentration using a partition coefficient of 0.78 for IAP. Optical density values from both films were converted to their respective radioactivity concentrations using known standards for ^{14}C. No attempt was made to calculate absolute rCBF values from HMPAO uptake.

RESULTS

With the exception of cortical hypoperfusion, which was most marked in the parietal cortex (side-to-side differences 50 ± 22 ml/100 g/min, $p = 0.019$) on the side of the craniotomy, nonseizure animals showed normal IAP uptake patterns (*15–18*). In seizure animals, there were significant flow increases in the areas where penicillin was injected (mean side-to-side difference 170 ml/100 g/min, $p = 0.035$) (Fig. 1): the ipsilateral thalamus, principally in the dorsomedial nucleus (mean side-to-side difference 287 ml/100 g/min, $p = 0.001$) (Fig. 2); but also in the ventral nucleus (mean side-to-side difference 142 ml/100 g/min, $p = 0.003$), the substantia nigra pars reticularis (mean side-to-side difference 78 ml/100 g/min, $p = 0.007$) (Fig. 3); and the medial and lateral habenula (mean side-to-side differences 56 and 52 ml/100 g/min, $p = 0.008$ and 0.049, respectively). The absolute flows measured during the seizures included a maximum mean flow (over five animals with seizures) of 498 ml/100 g per min, with seven areas showing mean flows of over 300 ml/100 g/min. In individual animals, flows of more than 600 ml/100 g/min were discovered in 6 animals, between 400 and 600 ml/100 g/min in 13 and over 300 ml/100 g/min in 30.

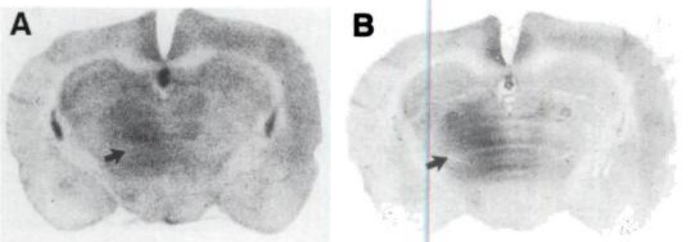

FIGURE 2. IAP (A) and HMPAO (B) images. Coronal section through the thalamus in animal 7, showing increased uptake of IAP and HMPAO in the thalamus ipsilateral to the focus (arrow), principally affecting the dorsomedial nucleus, but also affecting the ventral thalamic nucleus and, to a small degree, the contralateral medial thalamus. There is decreased uptake in the parietal cortex ipsilateral to the focus, and high HMPAO uptake relative to IAP can be seen in the choroid plexus (small arrow).

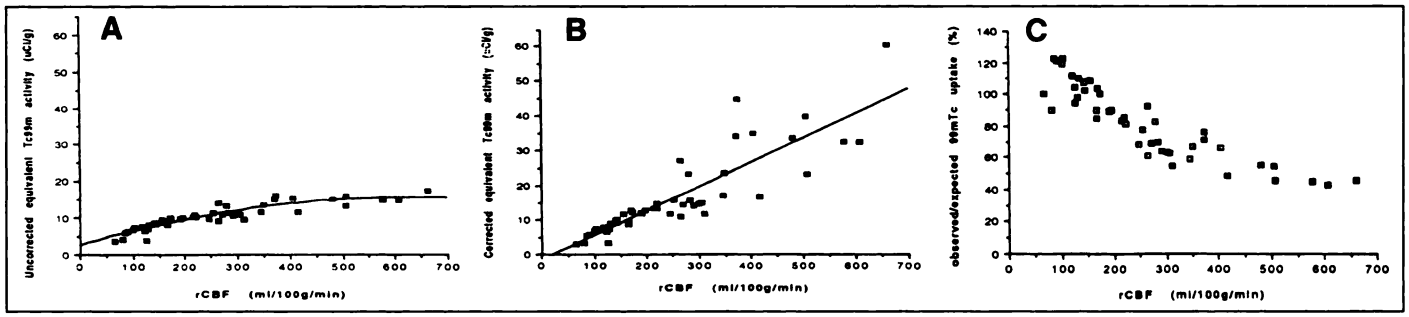

FIGURE 3. (A) Animal 8. Graph of uncorrected ^{99m}Tc equivalent activity versus rCBF as determined by the IAP method. A second-order polynmial fit is illustrated ($y = 2.75 + 4.01e - 2x - 3.13e - 5x^2$; $R^2 = 0.885$, $p < 0.001$). (B) Graph of the same data as in C after application of the Lassen correction to ^{99m}Tc equivalent activities. A straight line fit is illustrated ($y = -1.59 + 7.07e - 2x$; $R^2 = 0.872$, $p < 0.001$). (C) Graph of observed versus expected ^{99m}Tc uptake (%).

Correlation of Carbon-14-IAP and Technetium-99m-HMPAO Uptake

Uptake Patterns. HMPAO films displayed uptake patterns identical in detail to those on the IAP films. Areas of high flow were equally well visualised on HMPAO as on IAP films and normal gray and white matter structures were clearly separated on both.

Uptake differences were observed in two regions within the brain: (a) uptake in the choroid plexus was much higher in the HMPAO films in all 10 animals (Fig. 2) and (b) HMPAO uptake in one animal was relatively high in the supramamillary nucleus. In addition, there was also higher ^{99m}Tc activity in the rhinal and other fissures (Fig. 1).

There was little difference in spatial resolution between IAP and HMPAO films in general, although some image blurring was evident on the HMPAO films, probably due to the range of the higher energy electrons emitted by ^{99m}Tc.

Correlation between rCBF and HMPAO Uptake. An example of the correlation between the observed ^{99m}Tc activity and rCBF is shown in Figure 4A. The same data with the Lassen correction applied to ^{99m}Tc uptake are shown in Figure 4B. Observed (uncorrected) versus expected ^{99m}Tc activity for the same animal is shown in Figure 4C.

The current data show an expected curvilinear relationship between ^{99m}Tc uptake and a falloff in the rate of increase of ^{99m}Tc uptake. Application of the Lassen correction produces a more linear relationship which appears to have been achieved given the cost of increased scatter at high flows. All animals showed the same results, and no ^{99m}Tc activity levels fell as very high flows were reached. The R^2 values for straight line fits ranged from 0.740–0.944 ($p < 0.001$ in all animals). At lower flow levels, the relationship between ^{99m}Tc uptake and flow was approximately linear, and remained so in the majority of the animals up to 200 ml/100 g/min.

DISCUSSION

Experimental Protocol

Generalized experimental seizures in rats have produced CBF elevations of up to 900% with respect to resting levels of flow (*10,19,20*). There is no good quantitative data on the magnitude of rCBF rise during focal seizures in man, however, largely because of methodological difficulties. In the present study, flows were seen as high as 717 ml/100 g per min, which if seen in man, would represent a 7%–900% increase (*21–23*). Thus, it seems likely that the flows achieved in this study were sufficiently high to encompass the probable range of flows in focal epilepsy in humans.

For HMPAO backdiffusion to occur, cerebral circulation must continue to function after the first pass through brain tissue after injection. In this study, HMPAO was administered 3.5–4.5 min before the animal, was sacrificed, i.e., six times the half-life of the conversion of HMPAO from a lipophilic to hydrophilic compound. This time frame allowed a more than 98% of the HMPAO delivered to the brain on first pass to be converted, assuming there was no washout. A shorter time period would have had the advantage of allowing IAP to be measured closer to the HMPAO injection, but would not have allowed cerebral neuronal HMPAO levels to stabilize. All animals were in a steady state during this period, and our experimental protocol assumes that cerebral circulation was also in steady state.

This study used a double-label technique which resulted in a small amount of cross-contamination of the HMPAO and IAP films. In fact, contamination of IAP films by ^{99m}Tc activity is very small. Over a period of 4 days, ^{99m}Tc (half-life 6 hr) activity falls to 0.0015% of original levels. By the time the area with the highest ^{99m}Tc activity seen in this study was exposed on ^{14}C film, its activity was 0.001 kBq/g, a figure which continued to decrease by half every 6 hr during the 2 wk of exposure of the ^{14}C films. This would result in negligible contamination of the IAP film.

The contamination of ^{99m}Tc films by ^{14}C can be illustrated by the following examples. The maximum activity seen on the IAP films in the present study was 42kBq/g, in a structure (ipsilateral dorsomedial thalamic nucleus, animal 7) which had a ^{99m}Tc activity of 663kBq/g (in ^{14}C equivalent units). The [^{14}C]IAP contamination of the HMPAO film in this structure was therefore 6.3% at maximum. In an area of low flow (left subcortical white matter, animal 2), the [^{14}C]IAP activity was 7.2kBq/g, and the ^{99m}Tc equivalent activity 135 kBq/g. Contamination in this instance was 5.3% at maximum. Contamination would be higher if an area with a low uptake in the HMPAO film had a high uptake in the IAP film, but such discordance did not occur in the present study.

Technetium-99m activity was measured in ^{14}C equivalent units because of the practical difficulties of establishing standards with such a short-lived radionuclide. Although the film was exposed to higher energy electrons with ^{99m}Tc than with ^{14}C, the use of ^{14}C standards as a reference for other radionuclides has been validated by Lear et al. (*24*) for a range of ^{14}C activities similar to the standards used in the present study. None of the ^{99m}Tc measurements exceeded the highest ^{14}C standard.

Correlation between HMPAO and IAP Uptake

Although there was a falloff in the rate of increase in HMPAO uptake at very high flow levels, HMPAO uptake did not begin to fall as flow increased in any animals. The results therefore show that the delivery of HMPAO during the first

pass continues to be the dominant factor in the final distribution of the tracer, although high flows are relatively underestimated. The proportion of the tracer retained in brain tissue falls at high flows (Fig. 4C), but the relationship tends to plateau at these levels. This raises the possibility that the trapping mechanism has a component with a half-life much shorter than 40 sec.

The correlation between CBF and HMPAO uptake is less close in the present study than that found in a previous study. Bullock et al. (*4*) found R^2 values of 0.84–0.93 using pooled data from 11 rats, and correlated flow as measured by IAP and HMPAO uptake at different stages of acute focal ischemia. Flows as high as 300 ml/100 g per min were recorded. This compares with the range of R^2 valve of 0.74–0.94 for individual animals in the present study, where the range of flows was two times greater. The range of flows may have some bearing on this difference, as the spread of data became greater at high flows in most animals, more so after application of the Lassen correction. The Lassen correction and the calculation of flow from IAP activity both tend to magnify small errors in densitometry as flows increase (*20*). Postmortem diffusion of IAP from areas of high to low flow might also be a contributory factor (*25*), as the magnitude of this effect will vary according to whether or not there is a low-flow area adjacent to the point of measurement.

Distribution of HMPAO as indicated by the autoradiographs was almost identical to that of IAP. The relatively high ^{99m}Tc uptake seen in the choroid plexus has been noted previously (*4*), and is probably due to concentration of unbound ^{99m}Tc pertechnetate by this structure. Similarly, the high activity seen in the rhinal and other fissures (Fig. 1) may be due to ^{99m}Tc either in the CSF or in the pia, which will have decayed by the time of the ^{14}C exposure. There is no ready explanation for the difference seen between IAP and HMPAO uptake in the supramamillary nucleus in animal 6. The supramammillary nucleus has not been noted to be involved in seizure activity in previous animal studies of local metabolic rate using the penicillin model of focal motor seizures (*26–29*).

CONCLUSION

HMPAO-SPECT is primarily an imaging technique. In practice, nonlinear color scales are universally used to display the images. It is not therefore of primary importance that there is a strictly linear relationship between tracer uptake and rCBF. It is, however, important that there is a unique tracer uptake value for each flow rate, and that tracer uptake increases as flow does. This study confirms that this is the case for ^{99m}Tc HMPAO at cerebral blood flows up to ten times normal human values. This result also suggests that HMPAO-SPECT is capable of imaging the increases in cerebral blood flow that occur during focal seizure activity.

ACKNOWLEDGMENTS

This study was supported by the Wellcome Surgical Institute, Garscube Estate, Glasgow. We thank Professor J. McCulloch, head of the Neuroscience Group, for his support.

REFERENCES

1. Neirinckx RD, Canning LR, Piper IM, et al. Technetium 99m d,l-HMPAO: a new radiopharmaceutical for SPECT imaging of regional cerebral blood perfusion. *J Nucl Med* 1987;28:191–202.
2. Costa DC, Jones BE, Steiner TJ, et al. Relative ^{99m}Tc HMPAO and ^{113}Sn microspheres distribution in dog brain. *Nuklearmedizin* 1987;23(suppl):498–500.
3. Lear JL. Initial cerebral HMPAO distribution compared to LCBF: use of a model which considers cerebral HMPAO trapping kinetics. *J Cereb Blood Flow Metab* 1988;8(suppl 1):S31–S37.
4. Bullock R, Patterson J, Park C. Evaluation of ^{99m}Tc-hexamethylpropyleneamine oxime cerebral blood flow mapping after acute focal ischaemia in rats. *Stroke* 1991;22:1284–1290.
5. Lassen NA, Andersen AR, Freiberg L, Paulson OB. The retention of ^{99m}Tc/DL-HMPAO in human brain after intracarotid bolus injection: a kinetic analysis. *J Cereb Blood Flow Metab* 1988;8:S13–S22.
6. Andersen AR, Friberg H, Knudsen GM. Extraction of ^{99m}Tc/DL-HMPAO across the blood-brain barrier. *J Cereb Blood Flow Metab* 1988;8 (suppl 1):S44–S51.
7. Andersen AR, Friberg H, Lassen NA, Kristensen K, Neirinck R. Assessment of the artererial input curve for ^{99m}Tc/DL-HMPAO by rapid octanol extraction. *J Cereb Blood Flow Metab* 1988;8(suppl 1):S23–S30.
8. Yonekura Y, Nishizawa S, Mukai T, et al. SPECT with ^{99m}Tc HMPAO compared with regional cerebral blood flow measured by PET: effects of linearization. *J Cereb Blood Flow Metab* 1988;8:S82–S89.
9. Inugami A, Kanno I, Uemura K, et al. Linearisation correction of ^{99m}Tc-labeled HMPAO image in terms of rCBF distribution: comparison to $^{15}C\ O_2$ inhalation steady state method measured by positron emission tomography. *J Cereb Blood Flow Metab* 1988;8:S52–S60.
10. Duncan R, Patterson J, Roberts R, Hadley DM, Bone I. Ictal/postictal SPECT in the localisation of complex partial seizures. *J Neurol Neurosurg Psychiat.* 1993;56:141–148.
11. Berkovic SF, Newton MR, Chiron C, Dulac O. Single-photon emission computed tomography In: Engel J, Jr., ed. *Surgical treatment of the epilepsies.* New York: Raven; 1993.
12. Meldrum BS, Nilsson B. Cerebral blood flow and metabolic rate early and late in prolonged epileptic seizures induced in rats by bicuculine. *Brain* 1976;99:523–542.
13. Sperling B, Lassen NA. Hyperfixation of HMPAO in subacute ischemic stroke leading to spuriously high estimates of cerebral blood flow by SPECT. *Stroke* 1993;24:193–194.
14. Sakadura O, Kennedy C, Jehle J, et al. Measurement of local cerebral blood flow with iodo ^{14}C antipyrine. *Am J Physiol* 1978;234:H59–H66.
15. Tamura A, Graham, DI, McCulloch J, Teasedale GM. Focal cerebral ischemia in the rat. I. Description of technique and early neuropathological consequences following middle cerebral artery occlusion. *J Cereb Blood Flow Metab* 1981;1:53–60.
16. McCulloch J, Kelly PAT, Grome JJ, Pickard JD. Local cerebral circulatory and metabolic effects of indomethacin. *Am J Physiol,* 1982;243:H416–H423.
17. McCulloch J, Kelly PAT, Ford I. Effect of apomorphine on the relationship between local cerebral glucose utilization and local cerebral blood flow with an appendix on its statistical analysis. *J Cereb Blood Flow Metab* 1982;2:487–499.
18. Mohamed AA, Mendelow AD, Teasdale GM, Harper AM, McCulloch J. Effect of the calcium antagonist nimodipine on local cerebral blood flow and metabolic coupling. *J Cereb Blood Flow Metab* 1985;5:26–33.
19. Ingvar M, Siesjo BK. Local blood flow and glucose consumption in the rat brain during sustained bicuculine induced seizures. *Acta Neurol Scand* 1983;68:129–144.
20. Horton RW, Meldrum BS, Pedley TA, McWilliam JR. Regional cerebral blood flow in the rat during prolonged seizure activity. *Brain Res* 1980;192:399–412.
21. Yamamoto M, Meyer JS, Sakai F, Yamaguchi F. Aging and cerebral vasodilator responses to hypercarbia. *Arch Neurol* 1980;37:489–496.
22. Melamed E, Lavy S, Bentin S, Cooper G, Rinot Y. Reduction in cerebral blood flow during normal aging in man. *Stroke* 1980;11:31–34.
23. Meyer JS, Ishihara N, Deshmukh VD, et al. Improved method for noninvasive measurement of regional cerebral blood flow by ^{133}Xe inhalation. Description of method and normal values obtained in healthy volunteers. *Stroke* 1978;9:195–204.
24. Lear JL, Ackermann R, Kameyama M, Carson R, Phelps M. Multiple radionuclide autoradiography in evaluation of cerebral function. *J Cereb Blood Flow Metab* 1984;4:264–269.
25. Williams JL, Shea M, Furlan AJ, Little JR, Jones SC. Importance of freezing time when iodoantipyrene is used for measurement of cerebral blood flow. *Am J Physiol* 1991;261:H252–H256.
26. Collins RC. Metabolic response to focal penicilin seizures in rat: spike discharge versus after discharge. *J Neurochem* 1976;27:1473–1482.
27. Collins RC, Kennedy C, Sokoloff L, Plum F. Metabolic anatomy of focal motor seizures. *Arch Neurol* 1976;33:536–542.
28. Collins RC. Use of cortical circuits during focal penicillin seizures: an autoradiographic study with ^{14}C-deoxyglucose. *Brain Res* 1978;150:487–501.
29. Collins RC. Kindling of neuroanatomic pathways during recurrent focal penicillin seizures. *Brain Res* 1978,150:503–517.